

## CONSTRAINING CHANGES IN THE PROTON-ELECTRON MASS RATIO WITH INVERSION AND ROTATIONAL LINES

NISSIM KANEKAR<sup>1</sup>

*Draft version April 1, 2024*

### ABSTRACT

We report deep Green Bank Telescope (GBT) spectroscopy in the redshifted NH<sub>3</sub> (1,1), CS 1-0 and H<sub>2</sub>CO 0<sub>00</sub>-1<sub>01</sub> lines from the  $z \sim 0.685$  absorber towards B0218+357. The inversion (NH<sub>3</sub>) and rotational (CS, H<sub>2</sub>CO) line frequencies have different dependences on the proton-electron mass ratio  $\mu$ , implying that a comparison between the line redshifts is sensitive to changes in  $\mu$ . A joint 3-component fit to the NH<sub>3</sub>, CS, and H<sub>2</sub>CO lines yields  $[\Delta\mu/\mu] = (-3.5 \pm 1.2) \times 10^{-7}$ , from  $z \sim 0.685$  to today, where the error includes systematic effects from comparing lines from different species and possible frequency-dependent source morphology. Two additional sources of systematic error remain, due to time variability in the source morphology and velocity offsets between nitrogen-bearing and carbon-bearing species. We find no statistically-significant ( $\geq 3\sigma$ ) evidence for changes in  $\mu$ , and obtain the stringent  $3\sigma$  constraint,  $[\Delta\mu/\mu] < 3.6 \times 10^{-7}$ , over 6.2 Gyrs; this is the best present limit on temporal changes in  $\mu$  from any technique, and for any lookback time, by a factor  $\gtrsim 5$ .

*Subject headings:* atomic processes — galaxies: high-redshift — quasars: absorption lines

### 1. INTRODUCTION

A generic prediction of theories that attempt to unify the standard model of particle physics with general relativity is that particle masses and low-energy coupling constants vary with space and time. A detection of such changes would imply new physics beyond the standard model. Tests of changes in fundamental “constants” such as the fine structure constant  $\alpha$ , the proton-electron mass ratio  $\mu$  or the proton g-factor  $g_p$  are hence of much interest (e.g. Uzan 2003).

Redshifted atomic and molecular spectral lines provide an interesting avenue to probe the possibility of fundamental constant evolution over cosmological timescales (Savedoff 1956). Comparisons between the redshifts of lines whose rest frequencies have different dependences on a constant like  $\alpha$  are sensitive to changes in the constant [see Kanekar (2008) for a recent review]. There are a number of such techniques, using comparisons between different transitions (e.g. Thompson 1975; Wolfe et al. 1976; Dzuba et al. 1999; Darling 2003; Chengalur & Kanekar 2003; Kanekar & Chengalur 2004; Flambaum & Kozlov 2007). Indeed, one of these techniques, the many-multiplet method, has yielded evidence for changes in  $\alpha$ : Murphy et al. (2004) obtained  $[\Delta\alpha/\alpha] = (-5.4 \pm 1.2) \times 10^{-6}$  from 143 absorbers with  $\langle z \rangle = 1.75$  (see also Murphy et al. 2003). This result has as yet been neither confirmed nor ruled out (e.g. Srianand et al. 2007; Molaro et al. 2008; Murphy et al. 2008b; Kanekar et al. 2010b), but evidence has now been found for additional systematic effects in the data, due to errors in the wavelength calibration (Griest et al. 2010). Recently, an independent technique, using radio “conjugate” satellite OH lines (Kanekar et al. 2004; Kanekar et al. 2005), found weak evidence (at  $\sim 99.1\%$  confidence level) for changes in a combination of  $\alpha$ ,  $\mu$  and  $g_p$ : Kanekar et al. (2010a) obtained  $[\Delta G/G] = (-1.18 \pm 0.46) \times 10^{-5}$  between  $z \sim 0.247$  and the present epoch, where  $G \equiv g_p[\mu\alpha^2]^{1.85}$ . If changes in  $\alpha$  are assumed to dominate over those in  $\mu$  and  $g_p$ ,

one obtains  $[\Delta\alpha/\alpha] = (-3.1 \pm 1.2) \times 10^{-6}$ , consistent with the result of Murphy et al. (2004), albeit at a lower redshift.

For three decades, ro-vibrational molecular hydrogen (H<sub>2</sub>) lines provided the sole method to directly probe changes in the proton-electron mass ratio (Thompson 1975). Unfortunately, few redshifted H<sub>2</sub> absorbers have been detected so far (e.g. Ledoux et al. 2003), and, of these, only four have been found suitable to study changes in  $\mu$  (e.g. Ivanchik et al. 2005; Reinhold et al. 2006; King et al. 2008; Thompson et al. 2009; Malec et al. 2010; Wendt & Molaro 2011). These results have also been controversial: Reinhold et al. (2006) obtained  $[\Delta\mu/\mu] = (+2.0 \pm 0.6) \times 10^{-5}$  from two absorbers at  $z \sim 2.6 - 3.0$ , i.e. evidence for a larger value of  $\mu$  at high redshift (see also Ivanchik et al. 2005). However, independent re-analyses of these data by King et al. (2008) and Thompson et al. (2009), using improved wavelength calibration techniques, found no evidence for changes in  $\mu$ . King et al. (2008) obtain  $[\Delta\mu/\mu] = (+2.6 \pm 3.0) \times 10^{-6}$  from three absorbers at  $z \sim 2.6 - 3.0$  (including the two systems of Reinhold et al. 2006); note, however, that Wendt & Molaro (2011) argue that systematic errors have been under-estimated in the latter analysis.

A new laboratory technique to probe changes in  $\mu$  was proposed by van Veldhoven et al. (2004), using inversion transitions of deuterated ammonia (ND<sub>3</sub>). Flambaum & Kozlov (2007) adapted this technique to astrophysical circumstances, using ammonia (NH<sub>3</sub>) inversion lines and rotational lines. Rotational and inversion line frequencies have different dependences on  $\mu$ , and a comparison between the redshifts of NH<sub>3</sub> inversion lines and rotational (e.g. CO, HCO<sup>+</sup>, CS, etc) lines from a single cosmologically-distant absorber is thus sensitive to changes in  $\mu$ . Only two redshifted NH<sub>3</sub> absorbers are currently known, at  $z \sim 0.685$  towards B0218+357 (Henkel et al. 2005) and  $z \sim 0.886$  towards B1830–210 (Henkel et al. 2008). In both cases, the NH<sub>3</sub> detection spectra have been used to obtain initial constraints on changes in  $\mu$  (Murphy et al. 2008a; Henkel et al. 2009). Finally, the ammonia technique has also been used to search for spatial changes in  $\mu$ : Levshakov et al. (2010) obtained the (conservative) con-

<sup>1</sup> Ramanujan Fellow, National Centre for Radio Astrophysics, TIFR, Ganeshkhind, Pune - 411007, India

straint  $[\Delta\mu/\mu] < 3 \times 10^{-8}$  from studies of multiple molecular clouds in the Galaxy.

The  $z \sim 0.685$  absorber towards B0218+357 has a far smaller velocity spread than the  $z \sim 0.886$  system towards B1830–210 (Wiklind & Combes 1995, 1996b), making it a better candidate for accurate redshift measurements. The carbon monosulfide (CS) 1-0 line [rest frequency: 48.990957(2) GHz; Kim & Yamamoto 2003] is a good rotational transition for the comparison with the NH<sub>3</sub> inversion lines because it is known to be unsaturated in the  $z \sim 0.685$  absorber (Combes et al. 1997) and it lies at a frequency relatively close to that of the NH<sub>3</sub> (1,1) lines. The formaldehyde (H<sub>2</sub>CO) 0<sub>00</sub>-1<sub>01</sub> line [rest frequency: 72.837948(10) GHz; Cornet & Winnewisser 1980] was chosen as a second rotational transition, to obtain an estimate of systematic effects in the above comparison; this too is known to be unsaturated in the  $z \sim 0.685$  absorber (Jethava et al. 2007). This *Letter* reports Green Bank Telescope (GBT) spectroscopy in the redshifted NH<sub>3</sub> (1,1), CS 1-0 and H<sub>2</sub>CO 0<sub>00</sub>-1<sub>01</sub> lines, that yield the best present constraints on changes in the proton-electron mass ratio.

## 2. OBSERVATIONS, DATA ANALYSIS AND RESULTS

The GBT observations of the NH<sub>3</sub> (1,1) and CS 1-0 lines at  $z \sim 0.685$  towards B0218+357 were carried out in January and August 2008 (proposals AGBT07C-016 and AGBT07C-054), using the Ku- and Ka-band receivers, respectively. A spectrum in the redshifted H<sub>2</sub>CO 0<sub>00</sub>-1<sub>01</sub> line was obtained in July 2008 with the GBT Q-band receiver, as part of an absorption survey of the  $z \sim 0.685$  galaxy (proposal AGBT07C-054). Bandpass calibration was carried out via beam-switching for the NH<sub>3</sub> observations, and with sub-reflector nodding for the higher-frequency CS and H<sub>2</sub>CO observations. Two polarizations were used for the observations of the NH<sub>3</sub> (Ku-band) and H<sub>2</sub>CO (Q-band) lines, and a single Ka-band polarization for the CS line. The total observing times were 6 hours (NH<sub>3</sub>), 1.5 hours (CS) and 3 hours (H<sub>2</sub>CO), with the NH<sub>3</sub> observations split into two observing sessions, in January and August 2008. Standard procedures in the packages DISH (for the NH<sub>3</sub> lines) and GBTIDL (for the CS and H<sub>2</sub>CO lines) were used to analyse the data. The final NH<sub>3</sub>, CS, and H<sub>2</sub>CO spectra are shown in Figs. 1[A], [B] and [C]; these have velocity resolutions of  $\sim 0.26$ , 0.12 and 2.8 km/s, respectively (after Hanning-smoothing and re-sampling), and root-mean-square noise values of  $\sim 0.00082$ , 0.0097 and 0.0026, in optical depth units, per independent velocity channel.

A GBT Ku-band search was also carried out for the CCS 1-0 transition at  $z \sim 0.685$ ; no absorption was detected at the redshifted CCS line frequency, with a  $3\sigma$  optical depth limit of  $\sim 0.0016$  per 4.2 km/s channel. The K- and Ku-band receivers were further used to search for redshifted NH<sub>3</sub> (1,1) absorption from two other redshifted molecular absorbers, at  $z \sim 0.247$  towards B1413+135 (Wiklind & Combes 1997) and  $z \sim 0.674$  towards B1504+377 (Wiklind & Combes 1996a), with no detected absorption in either case. The  $3\sigma$  optical depth limits were 0.00068 per 4 km/s channel (B1413+135) and 0.00061 per 4 km/s channel (B1504+377).

The test for changes in the proton-electron mass ratio  $\mu$  was carried out through a simultaneous fit to the NH<sub>3</sub> (1,1), CS 1-0 and H<sub>2</sub>CO 0<sub>00</sub>-1<sub>01</sub> spectra, using the package VPFIT<sup>2</sup>. The velocity structure in all optically-thin lines was assumed to

be the same, in both the number of absorbing ‘‘clouds’’ and their redshifts. Turbulence was assumed to be the dominant contributor to the line widths, which were hence tied together in the fit (Murphy et al. 2008a). The NH<sub>3</sub> hyperfine structure was included by assuming local thermodynamic equilibrium (LTE), with the hyperfine ratios taken from Table S1 of (Murphy et al. 2008a). Finally, the fit also included a single velocity offset between the spectral components in the inversion and rotational transitions, to account for a possible change in the proton-electron mass ratio.

A simultaneous multi-component Voigt profile fit was carried out to the three spectra of Fig. 1 with the above assumptions, aiming to minimize  $\chi^2_\nu$  by varying the fit parameters. A 3-component fit was found to yield  $\chi^2_\nu = 1.05$  and no evidence for structure in the residuals after subtracting out the fits to each spectrum (see the lower panels of Fig. 1). Specifically, a Kolmogorov-Smirnov rank-1 test found the fit residuals for all lines to be consistent with a normal distribution within  $\sim 1\sigma$  confidence. One- and two-component fits were found to yield both a larger  $\chi^2_\nu$  and clear non-Gaussian structure in the residual spectra. While increasing the number of spectral components to four did yield a marginally-lower  $\chi^2_\nu$  ( $\sim 1.02$ ), the additional spectral component was only weakly detected in the H<sub>2</sub>CO spectrum (at  $\lesssim 3\sigma$  significance) and was not visible in the NH<sub>3</sub> or CS transitions. A 3-component model thus appears to provide a good fit to the data; however, for completeness, results from the 4-component fit will also be mentioned below.

For the coupled 3-component model, the number of fit parameters is 16, three redshifts, three line widths, nine optical depths in the NH<sub>3</sub>, CS, and H<sub>2</sub>CO lines, and the velocity offset between the inversion and rotational transitions. The parameters of the best 3-component fit are listed in Table 1; the best-fit velocity offset is  $\Delta V = (-0.36 \pm 0.10)$  km/s, with the NH<sub>3</sub> lines blueshifted relative to the rotational lines. A similar result is obtained from the best-fit 4-component model,  $\Delta V = (-0.39 \pm 0.11)$  km/s. Similar results are also obtained from carrying out 3-component fits to the NH<sub>3</sub> and CS lines (i.e. without including the H<sub>2</sub>CO line), and to the NH<sub>3</sub> and H<sub>2</sub>CO lines (i.e. without the CS line).

To obtain an estimate of systematic effects, a similar 3-component fit was also carried out to the CS and H<sub>2</sub>CO rotational lines alone (i.e. *without* including the NH<sub>3</sub> inversion lines). This yielded a velocity offset of  $\delta V = (0.029 \pm 0.068)$  km/s, between the CS and H<sub>2</sub>CO lines. The  $1\sigma$  error obtained here, when comparing two rotational lines, will be used as an estimate of the systematic error due to local velocity offsets between different species in the absorber.

The fractional change in the proton-electron mass ratio  $\mu$  is related to the measured velocity offset between inversion and rotational lines  $\Delta V$  by the expression (Flambaum & Kozlov 2007)  $[\Delta\mu/\mu] = 0.289 [(z_{inv} - z_{rot})/(1 + \bar{z})] \approx 0.289 [\Delta V/c]$ , where  $z_{inv}$  and  $z_{rot}$  are, respectively, the inversion and rotational redshifts, and  $\bar{z}$  is their average. Our final velocity offset is  $\Delta V = [-0.36 \pm 0.10(stat.) \pm 0.068(syst.)]$  km/s; this yields  $[\Delta\mu/\mu] = [-3.47 \pm 0.96(stat.) \pm 0.66(syst.)] \times 10^{-7}$ . Adding the statistical and systematic errors in quadrature, we obtain  $[\Delta\mu/\mu] = (-3.5 \pm 1.2) \times 10^{-7}$ , between  $z \sim 0.685$  and the present epoch.

## 3. DISCUSSION

An excellent summary of the systematic effects inherent in the comparison between rotational and inversion lines in

<sup>2</sup> <http://www.ast.cam.ac.uk/ffc/vpfit.html>

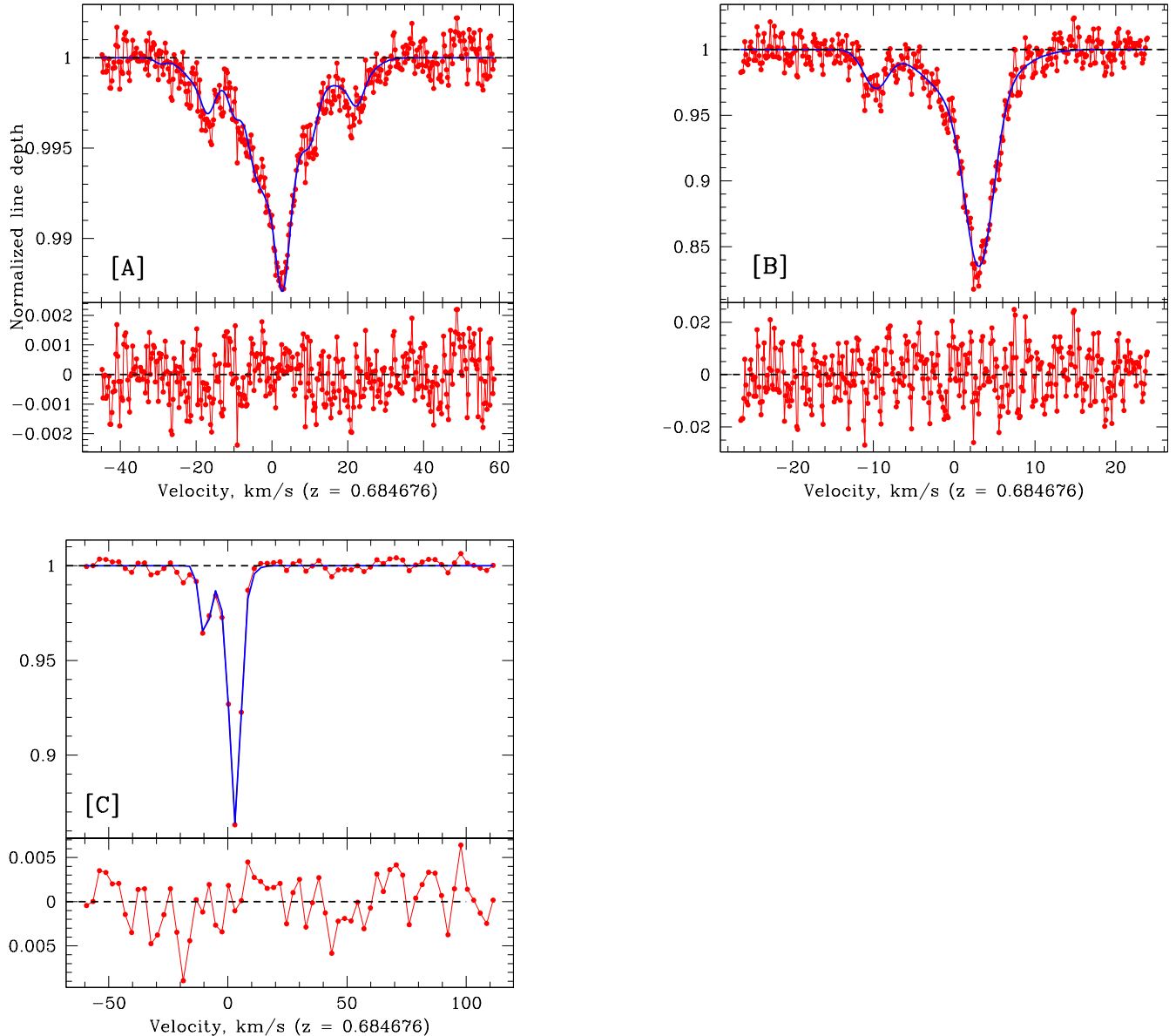


FIG. 1.— GBT spectra in the redshifted [A]  $\text{NH}_3$  (1,1), [B]  $\text{CS}$  1-0 and [C]  $\text{H}_2\text{CO}$   $0_{00}-1_{01}$  transitions from the  $z \sim 0.685$  absorber towards B0218+357. The upper panels show normalized line depth in each transition plotted against velocity, in km/s, relative to a heliocentric redshift of  $z = 0.684676$ ; the 3-component fit is overlaid on each spectrum. The lower panels show the residuals from the spectra after subtracting out the joint 3-component fit; these are consistent with noise.

the  $z \sim 0.685$  absorber is given by Murphy et al. (2008a). These include the following: (1) the assumption that different transitions have the same number of spectral components, and at the same redshifts, (2) the background source morphology is frequency-dependent, implying that the  $\text{NH}_3$  and rotational transitions might arise along slightly different sightlines, (3) the background source flux density (and hence morphology) varies with time, so observations at different epochs might probe different sightlines, (4) the assumption of LTE for the  $\text{NH}_3$  hyperfine structure, (5) saturation effects if highly-saturated lines [e.g. the  $\text{HCO}^+$  and  $\text{HCN}$  lines used by Murphy et al. (2008a)] are used, and (6) local velocity offsets between the species giving rise to the transitions. As noted by Murphy et al. (2008a), all these effects could yield significant contributions to their systematic errors. For example, the inversion and rotational transitions used by Murphy et al.

(2008a) were at very different frequencies,  $\sim 14$  GHz and  $\sim 106$  GHz; changes in the background source morphology could thus result in different sightlines in the different transitions. The  $\text{NH}_3$  and  $\text{HCO}^+/\text{HCN}$  observations were separated by a few years, implying that temporal variability in the source morphology could also be an issue, especially given that saturated transitions were used in the analysis. Finally, the  $\text{NH}_3$  spectra were of too low signal-to-noise ratio (S/N) to detect the  $\text{NH}_3$  hyperfine structure and to test for non-LTE effects.

Most of the above issues have been directly addressed in the present work. All three transitions used in the analysis are unsaturated and have been observed at high S/N, and with the same telescope. The two outlying  $\text{NH}_3$  hyperfine components (at  $\pm 19.5$  km/s relative to the strongest component) in the  $\text{NH}_3$  (1,1) line have also been clearly detected

Component	Velocity offset km/s	Redshift	FWHM km/s	Line depth $\times 100$		
				NH <sub>3</sub>	CS	H <sub>2</sub> CO
1	$(-0.36 \pm 0.10)$	0.6846935(2)	$3.99 \pm 0.13$	$0.496 \pm 0.060$	$13.83 \pm 0.78$	$15.61 \pm 0.84$
2		0.6846858(10)	$10.60 \pm 0.45$	$0.734 \pm 0.026$	$4.39 \pm 0.33$	$3.00 \pm 0.39$
3		0.6846214(7)	$3.53 \pm 0.33$	$0.128 \pm 0.032$	$2.84 \pm 0.28$	$5.17 \pm 0.37$

TABLE 1

PARAMETERS OF THE BEST 3-COMPONENT VOIGT PROFILE FIT TO THE NH<sub>3</sub> (1,1), CS 1-0 AND H<sub>2</sub>CO 0<sub>00</sub>-1<sub>01</sub> SPECTRA. THE SECOND COLUMN CONTAINS THE BEST-FIT VELOCITY OFFSET BETWEEN THE ROTATIONAL AND INVERSION LINES; NOTE THAT A SINGLE VELOCITY OFFSET WAS ASSUMED FOR ALL SPECTRAL COMPONENTS. THE REDSHIFTS OF COLUMN (3) ARE IN THE HELIOCENTRIC FRAME, WHILE THE LINE DEPTHS ( $\times 100$ ), LISTED IN THE LAST THREE COLUMNS, HAVE BEEN NORMALIZED BY THE SOURCE CONTINUUM AT EACH OBSERVING FREQUENCY.

(see Fig. 1[A]). As noted by Murphy et al. (2008a), non-LTE effects resulting in hyperfine “anomalies” should cause the satellite hyperfine components (with  $\Delta F_1 \neq 0$ , where  $F_1$  is the quadrupole quantum number) to have different optical depths. No evidence for such non-LTE conditions is apparent in the  $\pm 19.5$  km/s satellite hyperfine components in Fig. 1[A]; the optical depths are found to agree within the noise.

We note, finally, that the systematic error of  $7.6 \times 10^{-7}$  in the result of Murphy et al. (2008a) contains two contributions: (1)  $7 \times 10^{-7}$  because spectral components detected in the HCO<sup>+</sup> and HCN spectra may not be detected in the NH<sub>3</sub> spectra, due either to the large frequency difference between the inversion and rotation lines or to the fact that the HCO<sup>+</sup> and HCN lines are optically thick, and (2)  $3 \times 10^{-7}$  due to the possibility of non-LTE effects in the NH<sub>3</sub> spectra. Our choice of rotational lines and the higher sensitivity of our NH<sub>3</sub> spectra implies that neither of these are significant sources of systematic error in the present analysis.

Liszt et al. (2006) find that NH<sub>3</sub> column densities correlate best with CS and H<sub>2</sub>CO column densities in Galactic diffuse clouds; CS and H<sub>2</sub>CO are thus likely to be the best rotational transitions for the inversion/rotation comparison, as the correlation in column densities suggests that the three species are likely to arise in the same part of a gas cloud. Galactic absorption has also been detected in all three species towards two quasars, B0355+508 and B0415+379 (Liszt & Lucas 1995; Lucas & Liszt 1998; Liszt et al. 2006); both sightlines show two components in all species, with line velocities agreeing within 0.2 km/s [see Table 1 of Liszt & Lucas 1995, Table 6 of Lucas & Liszt 1998 and Table A1 of Liszt et al. 2006]; local velocity offsets between the species thus appear to be small. Further, the rotational and inversion line frequencies are much closer here than in the comparison of Murphy et al. (2008a), with the redshifted NH<sub>3</sub>, CS, and H<sub>2</sub>CO lines at  $\sim 14$  GHz,  $\sim 29$  GHz and  $\sim 43$  GHz, respectively. Changes in source morphology with frequency are thus a less important issue here than in the analysis of Murphy et al. (2008a). A direct test comes from the comparison between the two rotational lines, whose frequencies differ by a factor of  $\sim 1.5$ , comparable to the ratio of the CS and NH<sub>3</sub> frequencies ( $\sim 2$ ). The CS-H<sub>2</sub>CO comparison also provides an estimate of the systematic error due to local velocity offsets between different species in the clouds. This test found the CS and H<sub>2</sub>CO line redshifts to agree within the noise; the  $1\sigma$  error in this comparison has been used to quantify the systematic error due to both local velocity offsets and differing background source morphology at the different line frequencies. Finally, similar velocity offsets (consistent within the errors) were obtained in the independent comparisons between the NH<sub>3</sub> and CS lines, and the NH<sub>3</sub> and H<sub>2</sub>CO lines.

A source of systematic effects that could not be directly

addressed here is time variability in the background source morphology, which might yield different sightlines through the absorbing clouds at different epochs [Murphy et al. 2008a; see Muller & Guélin (2008) for the  $z \sim 0.886$  lens towards B1830–210]. Unfortunately, the redshifted NH<sub>3</sub>, CS and H<sub>2</sub>CO transitions towards B0218+357 require different GBT receivers and cannot be observed simultaneously. The present NH<sub>3</sub>, CS and H<sub>2</sub>CO observations were carried out between January and August 2008; the possibility that the weak offset between the inversion and rotational lines arises due to small changes in the sightline thus cannot be ruled out. Further, the agreement between CS and H<sub>2</sub>CO velocities does not rule out the possibility that nitrogen-bearing species like NH<sub>3</sub> arise at different velocities than carbon-bearing species like CS and H<sub>2</sub>CO. This can only be tested by using rotational transitions of other nitrogen-bearing species (e.g. HC<sub>3</sub>N, CH<sub>3</sub>CN, etc).

While there are two possible sources of systematic error that we are as yet unable to quantify, the present data show no statistically-significant ( $\geq 3\sigma$ ) evidence for changes in the proton-electron mass ratio. Our  $3\sigma$  upper limit on changes in  $\mu$  is  $[\Delta\mu/\mu] < 3.6 \times 10^{-7}$ , between  $z \sim 0.685$  and  $z = 0$  (a lookback time of 6.2 Gyrs). For comparison, Murphy et al. (2008a) obtained  $[\Delta\mu/\mu] < 1.8 \times 10^{-6}$  ( $2\sigma$ ) in the  $z \sim 0.685$  absorber towards B0218+357, while Henkel et al. (2009) obtained  $[\Delta\mu/\mu] < 1.4 \times 10^{-6}$  ( $3\sigma$ ) in the  $z \sim 0.886$  absorber towards B1830–210, with both results based on inversion/rotation comparisons. Note, however, that Henkel et al. (2009) used single-Gaussian fits for the NH<sub>3</sub> and HC<sub>3</sub>N lines towards B1830–210, although it is clear from the profiles of other unsaturated lines (e.g. CS) that at least three absorbing “clouds” are present along the sightline. Further, the GBT spectra in the strongest [(1,1), (2,2) and (3,3)] NH<sub>3</sub> lines towards B1830–210 were severely affected by radio frequency interference (see Fig. 1 of Henkel et al. 2008). The effect of these issues on the results of Henkel et al. (2009) is unclear, but the error budget is likely to increase. At higher redshifts, the best published constraint on changes in  $\mu$  is that of King et al. (2008):  $[\Delta\mu/\mu] < 6.0 \times 10^{-6}$ , using H<sub>2</sub> lines (but see Wendt & Molaro 2011). The present result,  $[\Delta\mu/\mu] < 3.6 \times 10^{-7}$  ( $3\sigma$ ) at  $z \sim 0.685$ , is thus the most sensitive constraint on temporal changes in  $\mu$  at any redshift, by a factor  $\gtrsim 5$ .

To compare this result with those from laboratory studies, it is necessary to assume a model for the variation of  $\mu$  with time. For linear variation, the present result yields  $\dot{\mu}/\mu < 5.6 \times 10^{-17}$  per year, more than an order of magnitude better than the best (model-dependent) laboratory constraint on changes in  $\mu$  (Rosenband et al. 2008).

In conclusion, we have used the GBT to obtain high S/N spectra in the NH<sub>3</sub> (1,1), CS 1-0 and H<sub>2</sub>CO 0<sub>00</sub>-1<sub>01</sub> transitions from the  $z \sim 0.685$  absorber towards

B0218+357. A comparison between the redshifts of the inversion and rotational lines yields a velocity offset of  $\Delta V = [-0.36 \pm 0.10(\text{stat.}) \pm 0.068(\text{syst.})]$  km/s, with the  $\text{NH}_3$  lines blueshifted relative to the rotational ones. Two sources of systematic error remain to be quantified, arising from (1) velocity offsets between nitrogen-bearing and carbon-bearing species, and (2) time variability in the background source morphology, which might yield different sightlines at different epochs. We find no statistically-significant ( $\geq 3\sigma$ ) evidence for changes in  $\mu$ , with the  $3\sigma$  constraint  $[\Delta\mu/\mu] < 3.6 \times 10^{-7}$  over a look-back time of 6.2 Gyrs. This is the strongest present constraint on temporal changes in the proton-electron mass ratio.

I thank Bob Carswell and Michael Murphy for much help with using VPFIT for the Voigt-profile fitting, Carl Bignell and Bob Garwood for help in the scheduling of the GBT observations and the GBT data analysis, and Dave Meier for permission to use the  $\text{H}_2\text{CO}$  line detected in our survey of B0218+357 for this project. I also acknowledge support from the Department of Science and Technology, India, via a Rammanujan Fellowship. The National Radio Astronomy Observatory is operated by Associated Universities, Inc, under cooperative agreement with the NSF.

## REFERENCES

- Chengalur, J. N. & Kanekar, N. 2003, *Phys. Rev. Lett.*, 91, 241302  
 Combes, F., Wiklind, T., & Nakai, N. 1997, *A&A*, 327, L17  
 Cornet, R. A. & Winnewisser, G. 1980, *J.Mol.Spec.*, 80, 438  
 Darling, J. 2003, *Phys. Rev. Lett.*, 91, 011301  
 Dzuba, V. A., Flambaum, V. V., & Webb, J. K. 1999, *Phys. Rev. Lett.*, 82, 888  
 Flambaum, V. V. & Kozlov, M. G. 2007, *Phys. Rev. Lett.*, 98, 240801  
 Griest, K., Whitmore, J. B., Wolfe, A. M., Prochaska, J. X., Howk, J. C., & Marcy, G. W. 2010, *ApJ*, 708, 158  
 Henkel, C., Braatz, J. A., Menten, K. M., & Ott, J. 2008, *A&A*, 485, 451  
 Henkel, C., Jethava, N., Kraus, A., Menten, K. M., Carilli, C. L., Grasshoff, M., Lubowich, D., & Reid, M. J. 2005, *A&A*, 440, 893  
 Henkel, C., Menten, K. M., Murphy, M. T., Jethava, N., Flambaum, V. V., Braatz, J. A., Muller, S., Ott, J., & Mao, R. Q. 2009, *A&A*, 500, 725  
 Ivanchik, A., Petitjean, P., Varshalovich, D., Aracil, B., Srianand, R., Chand, H., Ledoux, C., & Boissé, P. 2005, *A&A*, 440, 45  
 Jethava, N., Henkel, C., Menten, K. M., Carilli, C. L., & Reid, M. J. 2007, *A&A*, 472, 435  
 Kanekar, N. 2008, *Mod. Phys. Lett. A*, 23, 2711  
 Kanekar, N. & Chengalur, J. N. 2004, *MNRAS*, 350, L17  
 Kanekar, N., Chengalur, J. N., & Ghosh, T. 2004, *Phys. Rev. Lett.*, 93, 051302  
 —. 2010a, *ApJ*, 716, L23  
 Kanekar, N. et al. 2005, *Phys. Rev. Lett.*, 95, 261301  
 Kanekar, N., Prochaska, J. X., Ellison, S. L., & Chengalur, J. N. 2010b, *ApJ*, 712, L148  
 Kim, E. & Yamamoto, S. 2003, *J.Mol.Spec.*, 219, 296  
 King, J. A., Webb, J. K., Murphy, M. T., & Carswell, R. F. 2008, *Phys. Rev. Lett.*, 101, 251304  
 Ledoux, C., Petitjean, P., & Srianand, R. 2003, *MNRAS*, 346, 209  
 Levshakov, S. A., Molaro, P., Lapinov, A. V., Reimers, D., Henkel, C., & Sakai, T. 2010, *A&A*, 512, 44  
 Liszt, H. & Lucas, R. 1995, *A&A*, 299, 847  
 Liszt, H., Lucas, R., & Pety, J. 2006, *A&A*, 448, 253  
 Lucas, R. & Liszt, H. 1998, *A&A*, 337, 246  
 Malec, A. L., Buning, R., Murphy, M. T., Milutinovic, N., Ellison, S. L., Prochaska, J. X., Kaper, L., Tumlinson, J., Carswell, R. F., & Ubachs, W. 2010, *MNRAS*, 403, 1541  
 Molaro, P., Reimers, D., Agafonova, I. I., & Levshakov, S. A. 2008, *European Physical Journal Special Topics*, 163, 173  
 Muller, S. & Guélin, M. 2008, *A&A*, 491, 739  
 Murphy, M. T., Flambaum, V. V., Muller, S., & Henkel, C. 2008a, *Science*, 320, 1611  
 Murphy, M. T., Flambaum, V. V., Webb, J. K., Dzuba, V. V., Prochaska, J. X., & Wolfe, A. M. 2004, in *Lecture Notes in Physics*, Vol. 648, *Astrophysics, Clocks and Fundamental Constants*, ed. S. G. Karshenboim & E. Peik (Berlin: Springer-Verlag), 131  
 Murphy, M. T., Webb, J. K., & Flambaum, V. V. 2003, *MNRAS*, 345, 609  
 Murphy, M. T., Webb, J. K., & Flambaum, V. V. 2008b, *MNRAS*, 384, 1053  
 Reinhold, E., Buning, R., Hollenstein, U., Ivanchik, A., Petitjean, P., & Ubachs, W. 2006, *Phys. Rev. Lett.*, 96, 151101  
 Rosenband, T. et al. 2008, *Science*, 319, 1808  
 Savedoff, M. P. 1956, *Nature*, 178, 688  
 Srianand, R., Chand, H., Petitjean, P., & Aracil, B. 2007, *Phys. Rev. Lett.*, 99, 239002  
 Thompson, R. I. 1975, *ApL*, 16, 3  
 Thompson, R. I., Bechtold, J., Black, J. H., Eisenstein, D., Fan, X., Kennicutt, R. C., Martins, C., Prochaska, J. X., & Shirley, Y. L. 2009, *ApJ*, 703, 1648  
 Uzan, J.-P. 2003, *Rev. Mod. Phys.*, 75, 403  
 van Veldhoven, J., Küpper, J., Bethlem, H. L., Sartakov, B., van Roij, A. J. A., & Meijer, G. 2004, *Eur. Phys. Jour. D*, 31, 337  
 Wendt, M. & Molaro, P. 2010, *A&A*, 526, 96  
 Wiklind, T. & Combes, F. 1995, *A&A*, 299, 382  
 —. 1996a, *A&A*, 315, 86  
 —. 1996b, *Nature*, 379, 139  
 —. 1997, *A&A*, 328, 48  
 Wolfe, A. M., Broderick, J. J., Condon, J. J., & Johnston, K. J. 1976, *ApJ*, 208, L47